

# Transient Stability Improvement of an Integrated Grid using STATCOM

<sup>1</sup>D. Reddy Sekhar Naidu, <sup>2</sup>K. V. Satheesh babu, <sup>3</sup>S. Khadar Vali

<sup>1</sup>Department of electrical and electronic engineering, Madanapalle institute of technology and science, Madanapalle

<sup>2</sup>Department of electrical and electronic engineering, Madanapalle institute of technology and science, Madanapalle

<sup>3</sup>Department of electrical and electronic engineering, Madanapalle institute of technology and science, Madanapalle

**Abstract:** By using STATCOM, voltage is controlled plus damping upgrading of a grid associated offshore wind farm, marine current farm and photovoltaic plant [1]. Doubly fed induction motor motivated by wind turbine is used to simulate the results and presentation of the offshore wind farm. Marine current farm is simulated with squirrel cage induction generator which is determined through correspondent marine-current turbine. Photovoltaic plant is simulated by modules those are associated in series and parallel to the inverter. To achieve effective damping by using the theory of modal control STATCOM is designed with a damping controller [5]. This designed STATCOM is used to study the system under various conditions. To simulate the effectiveness of method a frequency-domain scheme which is support on a linear zed structure model with Eigen value and a time-domain approach which depend on nonlinear system arc employed. STATCOM which is designed by damping controller is extremely effective and the system was calculated and results are simulated under various disturbance. The fluctuation in voltage in the ac bus which arises due to active power variations of the calculated system is too controlled to a maximum extent by using the STATCOM which is specially designed by damping controller [7].

## I. INTRODUCTION

Since major portion of the earth surface is covered by oceans and sun energy which leads to discovery of generation of power from sea-shores and sun temperature. A hybrid power generation which includes; power generation by off-shore wind farm (OWF), marine current farm (MCF) and photovoltaic be able to place at various locations across the globe. Generators motivated by marine-current turbine (MCT), offshore producers motivated through wind turbine (WT) combined with photovoltaic plant will develop into an original scheme for power construction in the prospect [3]. A hybrid power production scheme include offshore wind farm (OWF), marine-current farm (MCF) and photovoltaic be able to be widely expand at the exact place of the world in the hope. Solitary of the easy process of organization an OWF is to join the amount produced terminals of some DFIGs mutually also then attach to a power grid throughout an offshore step-up transformer with underwater cables.

To dart a MCF might perhaps utilize a few squirrel-confine incitement related unashamedly to the force lattice all during a seaward venture up transformer and undersea links. Commonly Wts and Mcts have to a great degree practically identical working

attributes however a SCIG-based MCF oblige touchy force for charge still as a DFIG base OWF with two bi-directional force converters can deal with its yield force element to be close up to solidarity. A Photovoltaic (PV) cells are used to change the sunlight into direct current (DC). Due to the short voltages and current generated in a PV cell several PV cells are linked in series and then in parallel to form a PV module for preferred output. The modules in a PV array are generally first linked in series to gain the preferred voltages and individual strings are then linked in parallel to let the system to generate more current. A three phase inverter is then associated to the PV modules for the power translation from dc to ac and a step up transformer to equal the grid voltages. At the point when the created dynamic force of a SCIG-based MCF is different because of marine-current changes, the captivated touchy force also the terminal voltage of the MCF might be widely influenced. In the experience of climbing matrix flimsiness, e.g., framework blame, a vitality storeroom framework or a manage machine used for a real high limit power production framework is normally needed to adjust fluctuating segments while linking to a force lattice [2].

A major OWF may join through distinctive FACTS gadgets or else vitality stockpiling frameworks, for example, a STATCOM, and so forth. The broke down result of security upgrade of force frameworks utilizing Statcoms along with the damping manager arrangement of Statcoms are advertised. The arrangement of a yield input direct quadratic controller used for a STATCOM with a variably cutting edge field of a wind vitality transformation framework to execute mutually voltage organizes and mechanical force organizes underneath lattice affiliation or islanding circumstance. Framework displaying and controller plan for quick load voltage guideline plus relief of voltage flash utilizing a STATCOM was built. Another D-STATCOM oversee calculation empower separation control of positive- and negative-arrangement ebbs as well as flows was arranged, and the calculation was focused around the created scientific form in the directions designed for a D-STATCOM working below unequal circumstance. An inside and out examination of the element execution of a STATCOM Furthermore a static synchronous series compensator (SSSC) with advanced reenactments was carry out [10]. The result of a learn on the submission of the freshly created STATCOM on behalf of the damping of torsion motions happen in an arrangement compensated air conditioning framework was computed whilst dynamic execution of the nonlinear framework through an enhanced STATCOM regulator was assessed in a three-stage flaw situation. Examination and similitude of distinctive control strategies, for example, PSS, static VAR compensator (SVC) and STATCOM for damping undesirable entomb zone motions in force frameworks were done. The ordinary technique for PI manage intended for a STATCOM was looked in, out with all around with distinctive input manage systems, and a straight best control focused around LQR control

was demonstrating to be prevalent as far as answer profile and oversee exertion fundamental. A STATCOM focused around a current-source inverter (CSI) was arranged, plus the nonlinear form of the CSI was modified to be a direct form amid a novel demonstrating procedure. The implicit STATCOM/BESS was presented used for the upgrading of dynamic with transient dependability also transmission capacity. The presentation of the diverse Certainties/BESS consolidations was looked at also gave investigational confirmation of the planned controls on a scaled STATCOM/BESS framework. An element voltage control plan focused around a gathering of SVC plus STATCOM innovation on a joined transmission framework through Igs in a wind homestead was examined [12].

Here is arranged as beneath. The arrangement and the utilized models for the computed incorporated OWF, MCF and photovoltaic among STATCOM are presented earliest. At that point, the configuration strategy plus outline outcome for the PID damping regulator of the planned STATCOM utilizing shaft arrangement method are portrayed. The transient soundness beneath three-stage short out shortcoming at the lattice is portrayed in this paper. At long last, correct crucial finishes of this paper are strained.

## II. MODELS OF THE STUIDED INTEGRATED OWF, MCF ALSO PV PLANT

Fig. 1 demonstrates the outline of the examined incorporated DFIG support OWF additionally SCIG support MCF and photovoltaic framework through the planned STATCOM. The OWF is spoken to through an enormous proportional accumulated DFIG determined by an equal totaled variably speed WT through a proportionate amassed gearbox [6]. The MCF is spoken to by a gigantic proportionate totaled SCIG determined by an identical amassed alterable velocity MCT from start to finish through an equal accumulated gearbox. The OWF, the MCF, the STATCOM with a neighborhood burden are joined toward an AC transport so as to is sustained to the inland power matrix during a seaward venture up transformer plus undersea links. The utilized factual replicas of the computed framework are portrayed as underneath.

### A. Wind Turbine

The power (in W) formed by a WT be able to spoken by

$$P_{mw} = \frac{1}{2} \rho_w \cdot A_{rw} \cdot V_w^3 \cdot C_{pw}(\lambda_w, \beta_w) \quad (1)$$

Here  $\rho$  be the air thickness in kilograms for every cubic meter ( $\rho = 1.225$ ),  $A_r$  is the edge drive part in square meters,  $V_w$  is the wind speed in meters for every second,  $C_{pw}$  is the force Coefficient of the WT.  $\lambda_w$  is the tip velocity degree of WT,  $\beta_w$  is cutting edge contribute plot of WT degrees. The wind speed is model the same as the arithmetical measure of a found wind velocity, a draft wind velocity, a slope wind velocity, and a commotion wind speed. The full mathematical statements for these four wind velocity apparatuses might be alluded to [17] even as the force coefficient of the WT is determined by [18]. The cut in, evaluated, also remove wind velocities of the computed WT are 4, 15, and 24 m/s, correspondingly. At the point when  $V_w$  is lesser than the evaluated wind speed

of the WT ( $V_{wrated}$ ),  $\beta_w = 0$ . At the point when  $V_w > V_{wrated}$ , the contribute edge be charge of arrangement of the WT demonstrated in Fig. 2 initiates and the field plot of the WT ( $\beta_w$ ) expand. Fig. 3 demonstrates the qualities of the caught for every unit automatic force against the for every unit generator rotor velocity of one of the forty 2mw Wts of the examined OWF from slice in wind pace to appraised wind speed [19]. The best conceivable yield focuses in Fig. 3 are the perfect most extreme yield mechanical force of

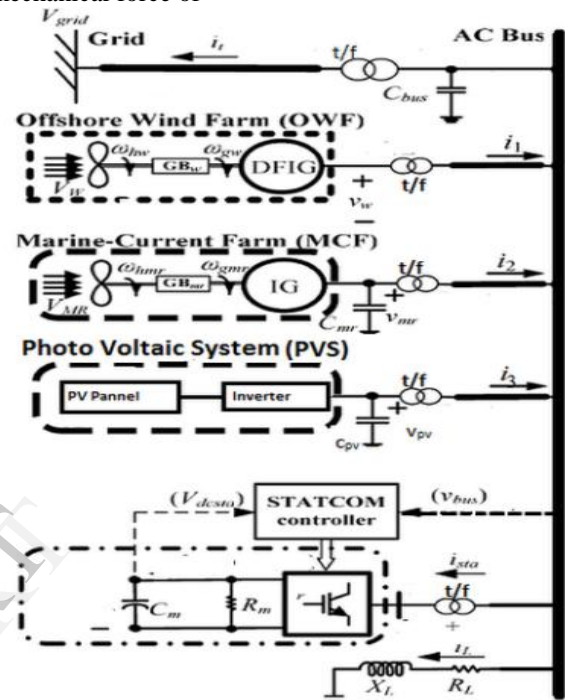


Fig.1.Design of the integrated OWF, MCF and PV system among STATCOM

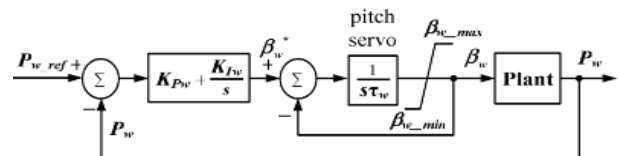


Fig.2.Diagram of the pitch angle manages system of the calculated WT.

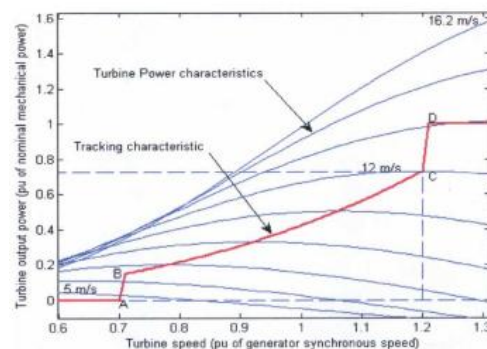


Fig.3.Turbine power vs. generator rotor speed characteristics.

### B. MASS SPRING DAMPER ARRANGEMENT WITH INDUCTION GENERATOR

Fig. 4 demonstrating the different inactivity outline request comparing mass spring damper reproduction of the WT

joined to the rotor shaft of the ascertained wind DFIG [16][18]. The reason for the identical gearbox (Gbw) among the WT plus the DFIG has been coordinated in this replica. The for every unit with pivot voltage current mathematical statements of a prompting producer might be alluded to [13], [14] also they could be use for the electrical branch of the wind DFIG plus the marine current SCIG

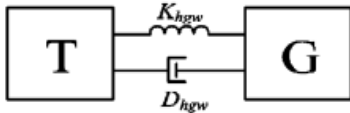


Fig.4 Two inactivity rundown request equal mass spring damper form of the WT connected to the rotor shaft of the computed wind DFIG.

C. DFIG POWER CONVERTER

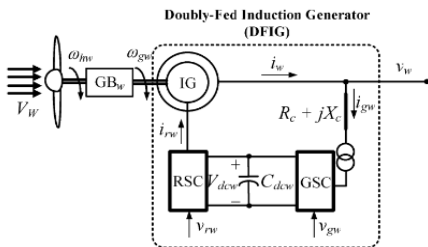


Fig.5. Single line figure of the calculated doubly fed induction generator.

Fig. 5 demonstrates the single line drawing of the mulled over wind DFIG. The wind DFIG stator windings are in a straight line associated to the low down voltage side of the 0.69/23kv stage asleep transformer even as interfaced by the rotor windings of the DFIG to the similar 0.69kv surface all during a rotor side converter (RSC), a DC join, a lattice region converter (GSC), a venture up transformer, in addition to a link line.

Intended for standard methodology of a wind DFIG, the information AC part voltage of the RSC plus the GSC could be proficiently controlled to get the points of synchronous yield dynamic force and receptive force control. Fig. 6 demonstrates the piece graph of the RSC of the contemplated DFIG. As demonstrated in Fig. 6. The procedure of the RSC obliges Iqrw and Idrw to track the variably proposal focuses that are dictated by keeping up the yield dynamic force and the stator slowing down at the circumstances values, correspondingly. The important voltage for the RSC (vrw) is resultant by conspiring the for every unit q and d-hub ebbs and flows of the RSC [27][29]. The oversee square outline of the GSC of the computed wind DFIG is uncovered in Fig. 7. The for every unit and hub ebbs and flows of the GSC, iqrw and idrw contain to track the circumstances focuses that are undaunted by keeping up the DC join voltage vdcw at the set worth and support of the yield of the GSC at solidarity force element, correspondingly. The essential for every unit voltage of the GSC (vgw) is coming about by computing the for every unit q and d hub flows of the GSC [20],[17].

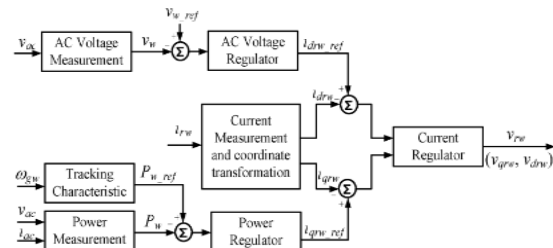


Fig. 6. RSC of the DFIG Control Block diagram.

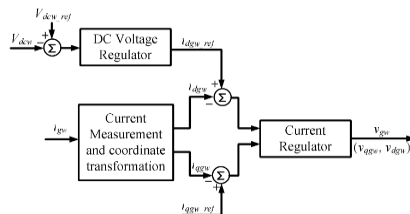


Fig. 7. GSC of the DFIG Control block diagram

D. MARINE CURRENT TURBINE PLUS MARINE CURRENT SPEED

The MCT is unsaid to be determined by wave speeds with the momentum speed is controlled in spring plus neap tides. The Marine momentum velocities are indicated at hourly interims opening at 6 h sooner than soaring waters and finale 6 h after. It is simple to determine a plain and useful model for marine flow speeds underneath the knowing tide coefficients as takes after:

$$V_{MR} = V_{nt} + \frac{(C_{mr} - 45)(V_{st} - V_{nt})}{95 - 45} \quad (2)$$

Here Cmr is the marine coefficient, 95 and 45 are the spring and neap tide medium coefficients, correspondingly, and Vst and additionally Vnt are the spring and neap marine-momentum speeds, correspondingly [2], [4]. The being used marine-current model is associating France to England region [2], [4]. The mechanical force (in W) produced by the considered MCT might be talked by

$$P_{mnr} = \frac{1}{2} \rho_{mr} \cdot A_{mr} \cdot V_{MR}^3 \cdot C_{pmr} (\lambda_{mr}, \beta_{mr}) \quad (3)$$

Here pmr is the salt water thickness in kg/m (pmr = 1025 kg/m<sup>3</sup>), Armr demonstrates the sharpened steel sway region in m<sup>2</sup>, VMR be the marine speed in m/s as portrayed in (2), and Cpmr is the force coefficient of the MCT. The cut- in, appraised, also cut-out paces of the mulled over MCT are 1, 2.5, and 4m/s, correspondingly. At the point when VMR is unrivaled than the appraised pace, the pitch- edge oversee arrangement of the MCT actuates to edge of the yield force of the MCT at the evaluated worth. Since the working turbine model, pitch-edge control framework, and mass-spring-damper model of the considered MCF are parallel to the ones that are in work in the OWF, some numerical models occupied with the OWF

might be sort of adjusted to be utilized within the MCF separated from the parameter

### E. PV SYSTEM MODEL

A Photovoltaic (PV) cells are used to translate the sunlight into direct current (DC). Due to the low voltages and current generated in a PV cell several PV cells are linked in sequence and then in similar to form a PV module for preferred output. The modules in a PV array are generally first joined in series to gain the desired voltages and individual strings are then attached in parallel to let the system to generate more current. The corresponding circuit of PV array is exposed in fig.1 [6] [8] [9].

From the fig.8.

$$I_A = (I_{ph} N_p) - I_{sh} - I_d \tag{4}$$

The array output current is a meaning of  $I_{ph}$ ,  $I_{sh}$  and  $I_d$ . The equations from (11) – (18) are the essential to design a solar PV array.

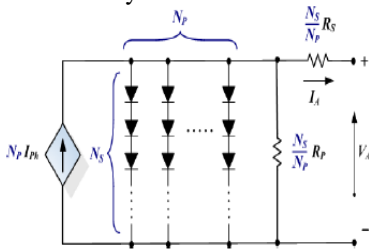


Fig.8. PV array Equivalent circuit

$$I_{ph} = I_{rr} (I_{sc} + K_1 (T_{op} - T_{ref}))$$

$$\left[ \frac{V + IR_S}{N_S} \right]$$

$$I_d = I_S N_P \left\{ \exp \left[ \frac{N_S}{n} \times V_T \times C \right] - 1 \right\}$$

$$V_T = \frac{KT_{OP}}{q} \tag{7}$$

$$I_S = I_{rs} \left[ \frac{T_{OP}}{T_{ref}} \right]^3 \left( \exp \frac{q^2 E_g}{Kn} \left( \frac{1}{T_{ref}} - \frac{1}{T_{op}} \right) \right) \tag{8}$$

$$I_{rs} = \frac{I_{sc}}{\exp \left( \frac{qV_{oc}}{KCT_{op}^n} \right)} - 1 \tag{9}$$

$$I_{Sh} = \frac{IR_S + V}{R_P} \tag{10}$$

$$V_T = \frac{KT_{OP}}{q} \tag{11}$$

Where

- $I_A$  PV array output current
- $I_{Ph}$  Solar cell photocurrent
- $I_{sh}$  Shunt current of PV array
- $I_d$  Diode current of PV array
- $N_p$  Number of modules in parallel
- $V_A$  Array output voltage
- $R_S$  Series resistance of the PV module
- $R_P$  Parallel resistance of the PV module
- $I_{rr}$  Cell reverse saturation current at temperature  $T_{ref}$
- $I_{sc}$  Short circuit current of the PVcell
- $K_1$  Short circuit current temperature coefficient
- $T_{op}$  Operating temperature of the PV cell in Kelvin's
- $T_{ref}$  Reference temperature of the PV cell in Kelvin's
- $I_S$  Reverse saturation current equation at  $T_{op}$
- $V_t$  Terminal voltage of the pv cell
- $I_{rs}$  Cell reverse saturation current at temperature  $T_{ref}$
- $E_G$  Band gap of the semiconductor used in the cell
- $K$  Boltzmann's constant,  $1.380658e - 23 \text{ J / K}$
- $q$  Electron charge,  $1.60217733e - 19 \text{ Cb}$
- $N_S$  Number of modules in series
- $N_p$  Number of modules in parallel
- $n$  P - N junction ideality factor
- $C$  Total number of cells in a PV module

In this term paper we are in view of a typical CS6P-250P PV modules along with SMA Solar Technology AG 1000 XT inverter.

### F. PV CONNECTED INVERTER

A three phase inverter is close to transmit out the power alteration of the array output power keen on AC power suitable for addition into the grid [19]. Pulse width modulation organize is one of the techniques used to form the phase of the inverter output voltage. The sinusoidal pulse-width modulation (SPWM) scheme generates a sinusoidal waveform by sorting an production pulse waveform among unstable width. An elevated switching frequency direct to a superior clean sinusoidal output waveform. The mainly wanted production voltage is accomplished by variable the frequency along with amplitude of a position otherwise modulating voltage. The differences during the amplitude with frequency of the orientation voltage modify the pulse-width models of the output voltage however maintain the sinusoidal modulation.

The modulation index [19] is clear as the percentage of the magnitude of amount produced voltage is produced by SPWM to the primary max out importance of the highest square wave. Consequently, the maximum modulation index of the SPWM method is

$$MI = \frac{V_{PWM}}{V_{\max-sixstep}} = \frac{\frac{V_{dc}}{2}}{\frac{2V_{dc}}{\pi}} = \frac{\pi}{4} \cong 0.7855 = 78.55\% \quad (12)$$

Here  $V_{PWM}$  is the greatest output voltage produced by a SPWM and  $V_{\max-sixstep}$  is the essential peak value of a square wave.

G.THE STATCOM

The block diagram of the considered STATCOM was exposed in Fig. 1. The per-unit q-and d-axis output voltages of STATCOM can be spoken by, correspondingly, [13]

$$V_{qsta} = V_{dcsta} . km . \cos(\theta_{bus} + \alpha) \quad (13)$$

$$v_{dsta} = V_{dcsta} . km . \sin(\theta_{bus} + \alpha) \quad (14)$$

Here  $V_{qsta}$  and  $V_{dsta}$  are the per-unit q also d axis voltages on the output fatal of the STATCOM, correspondingly,  $\theta_{bus}$  is the phase position of the AC-bus voltage,  $V_{dcsta}$  are the per unit DC voltage of the DC capacitor  $C_m$ , also  $km$  plus  $\alpha$  is the intonation index with phase position of the STATCOM, correspondingly. The per-unit DC voltage-current equation of the DC comparable capacitance  $C_m$  be able to writing as

$$(C_m) p(V_{dcsta}) = w_b [I_{dcsta} - (V_{dcsta} / R_m)] \quad (15)$$

Where

$$I_{dcsta} = i_{qsta} . km . \cos(\theta_{bus} + \alpha) + i_{dsta} . km . \sin(\theta_{bus} + \alpha) \quad (16)$$

Are the per unit DC current graceful into the +ve terminal of  $V_{dcsta}$  and  $R_m$  are the per-unit corresponding resistance that believe the comparable electrical sufferers of the STATCOM, with  $i_{qsta}$ ,  $i_{dsta}$  is the per- unit q also d axis currents graceful into the incurable of the STATCOM, correspondingly. The manage block diagram of the planned STATCOM with a PID damping regulator is given away in Fig. 9. The per-unit DC voltage  $V_{dcsta}$  forbidden by the phase angle  $\alpha$  as the voltage  $V_{staic}$  various by varying the modulation index  $km$ . The in use parameters of this essay are scheduled in Table I.

III. PID CONTROLLER DESIGN FOR STATCOM WITH MODERN CONTROL THEORY

This subdivision at hand a united move toward found on modal manage theory to plan the PID damping regulator of the planned STATCOM exposed in Fig. 9 for transient stability development of the calculated system.

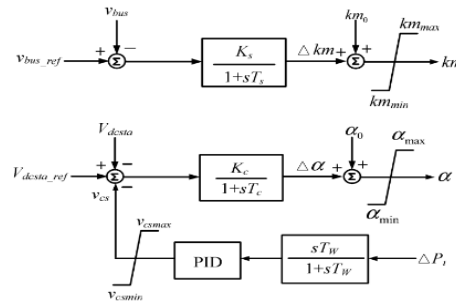


Fig. 9. Planned control STATCOM with the designed PID damping regulator

The nonlinear scheme equations expanded in Section II are foremost liberalized roughly a supposed working point to gain a set of liberalized system equation in matrix form of [30]

TABLE I: EMPLOYED SYSTEM PARAMETERS

System bases	
$V_{base}=690V, S_{base}=2MW, \omega_{base}=2\pi f_{base}, f_{base}=60Hz$	
Single WT-DFIG of the studied OWF	
$R_{sw}=0.00706pu, X_{sw}=0.171pu, r_{rw}=0.005pu$ $X_{rw}=0.156pu, X_{mw}=2.9pu, C_{dcw}=1.0pu$ $H_{gw}=0.5pu, H_{hw}=2.5pu, K_{hgw}=0.3pu, D_{hgw}=0.05pu$ $K_{pw}=10.2, K_{tw}=30.0, \tau_w=100s, \beta_{w\min}=0^0, \beta_{w\max}=30^0$	
Single MCT-SCIG of the studied MCF	
$R_{smr}=0.00488pu, X_{smr}=0.09241pu, r_{rmr}=0.00549pu$ $X_{mr}=0.09955pu, X_{mmr}=3.95279pu$ $H_{gmr}=0.5pu, H_{hmr}=3.5pu, K_{hgmr}=0.1pu, D_{hgmr}=0.1pu$ $K_{pmr}=20.0, K_{lmr}=30.0, \tau_{mr}=120s, \beta_{mr\min}=0^0, \beta_{mr\max}=30^0$	
PV module parameters	
$P_{max}=250w, PTC(W)=227.6W, V_{mpp}=30.1v, I_{mpp}=8.30A,$ $V_{oc}=37.2V, I_{sc}=8.87A$	
STATCOM(+/-32MVAR)	
$R_m=500pu, C_m=0.074F$ $R_{sta}=0.05pu, X_{sta}=0.2pu, T_s=0.01s, K_s=0.1$ $T_c=0.01s, K_c=0.5, km_{min}=0.0, km_0=0.5$ $\alpha_{max}=45^0, \alpha_{min}=-45^0, \alpha_0=0^0, v_{csmax}=0.2, v_{csmin}=-0.2$	
Transmission lines, capacitor banks, and local load	
$R_w=0.02pu, X_w=0.4pu$ $R_{mr}=0.02pu, X_{mr}=0.4pu, C_{mr}=0.3125pu$ $R_l=0.04pu, X_l=0.8pu, C_{bus}=0.125pu, R_c=8.0pu, X_l=4.0pu$	
Constants of power coefficients of WT , MCT and PV	
$C_1=0.34, c_2=128, c_3=0.4, c_4=c_5=0, c_6=11, c_7=10.9, c_8=0.08, c_9=0.01$ $d_1=0.18, d_2=85, d_3=0.38, d_4=0.25, d_5=0.5, d_6=10.2, d_7=6.2, d_8=0.025, d_9=-0.0443$	

$$PX = AX + BU + VW \quad (17)$$

$$Y = Cx + Du \quad (18)$$

Here X is the state vector and Y is the yield vector and also U is the outside or repair info vector, W is the inconvenience data vector in spite of the fact that A, b, C and D are all consistent grids of suitable size. To arrange a damping controller for the arranged STATCOM, the inconvenience info vector W in (8) and the outer commitment vector U in (9) could accurately surrendered by leasing  $D=V=0$ . The vector X know how to be parceled intrigued by 5 sub state vectors as

$X = [ X_{dfig}, X_{SCIG}, X_{MECH}, X_{ELEC}, X_{sta} ]^T$ , here  $X_{DFIG}$ , and  $X_{SCIG}$ ,  $X_{MECH}$ ,  $X_{ELEC}$ , also  $X_{STA}$  be the framework vectors of the wind DFIG, the marine-current SCIG, the programmed frameworks of mutually WT in addition to MCT, the electrical plan incorporate the AC transport, three transmission lines with nearby load, with the STATCOM, correspondingly. Since VW sometimes achieve the appraised wind speed of 15 m/s and VMR from time to time work over the evaluated marine-current rate of 2.5 m/s and in addition VW of 12 m/s and VMR of 2.5 m/s are effectively picked as the working focuses for conspiring the PID chief of the STATCOM. The Eigen values in addition to relating damping degrees of the considered included OWF and MCF not including plus among the STATCOM beneath  $VW = 12$  m/s and  $VMR = 2.5$  m/s are booked in the 3<sup>rd</sup> and the 4<sup>th</sup> segment of Table, correspondingly. The Eigen values  $\lambda_1 - \lambda_4$  and  $\lambda_5 - \lambda_8$  planned in chart I describe to the electrical forms of the considered DFIG and SCIG, correspondingly. The eigenvalues  $\lambda_9 - \lambda_{18}$  and  $\lambda_{19} - \lambda_{24}$  planned in chart I submitted the programmed modes and the electrical modes of the computed framework, correspondingly. The Eigen values  $\lambda_{25} - \lambda_{29}$  pass on to the modes of the STATCOM. A review of the Eigen qualities booked in chart I has the ensuing focuses. 1) The DFIG type, the SCIG type, and the electrical modes of the arranged framework are about altered on the troublesome plane; 2) the damping of together  $\lambda_{9,10}$  and  $\lambda_{11,12}$  is sort of upgraded when the STATCOM is connected to the coordinated OWF, MCF and PV framework. The damping of together  $\lambda_{9,10}$  and  $\lambda_{11,12}$  could be successively upgraded by the including of the arranged PID supervisor, 3). The whole framework Eigen qualities is arranged on the left 50% of the complex plane beneath a settled wind speed and an altered marine-current pace. The control square figure of the stage plot  $\alpha$  of the STATCOM together with the PID regulator was uncovered in Fig. 8. It is looking that the PID regulator utilizes the dynamic force variety of the transmission line ( $\Delta P_t$ ) as a crit damping indicator  $V_{cs}$  in regulate that the damping characteristics of the weakly damped modes  $\lambda_{9,10}$  as well as  $\lambda_{11,12}$  scheduled in chart I can be efficiently enhanced. For this reason, the o/p signal in (9) is  $Y = (\Delta P_t)$  and  $U = V_{cs}$  be the vector input. The  $H(s)$  of the planned PID regulator in s area is specified by

$$H(s) = \frac{U(s)}{Y(s)} = \frac{v_{cs}(s)}{\Delta P_t(s)} = \frac{sT_w}{1+sT_w} \left( K_p + \frac{K_I}{s} + sK_D \right) \quad (19)$$

Here  $T_w$  is time steady of the wash-out term as  $K_p$ ,  $K_I$  and  $K_D$  are the corresponding, and basic, and subordinate additions of the damping controller, correspondingly. Charming the Laplace change of (8)–(9), an arithmetical

comparison of the shut circle framework enclosing the PID controller could be acquired. The information motion in space could be talked by

$$U(s) = H(s)\Delta P_t(s) = H(s)Y(s) = H(s)CX(s) \quad (20)$$

Join together (10)&(11), then we got

$$sX(s) = \{A + B[H(s)C]\}X(s) \quad (21)$$

The trademark comparison of the shut circle framework together with the PID regulator is known by

$$\det\{sI - [A + BH(s)C]\} = 0 \quad (22)$$

The 4 limitations of the PID regulator could be fearless by substitute 2 sets of the specific complex and conjugated Eigen qualities matching to the appointed types ( $\lambda_9, 10$  and  $\lambda_{11, 12}$ ) interested in (13). The arrangement conclusions of the PID regulator of the STATCOM are realistic as under. Particular Eigen values:  $\lambda_{9,10} = -5.5 \pm j4.8$ ,  $\lambda_{11, 12} = -15.5 \pm j0.56$ . limitations of the arranged PID regulator:  $K_p=10.5, k_i=2.37, K_D=0.06, T_w=0.08$ s. The framework eigen estimations of the figured included OWF, MCF and PV framework among the arranged STATCOM appended among the arranged PID regulator are booked in the fifth segment of chart I. It might be obviously experiential that mutually  $\lambda_{9,10}$  and  $\lambda_{11, 12}$  have been accurately arranged on the favored areas on the troublesome plane. Some principle demands for choosing the doled out Eigen qualities are neatly portrayed as under [20]. 1) the acquired parameters of the PID damping regulator must be sensible. On the off chance that, the time consistent of the washout term ought to be sure and the additions of the PID regulator must be as little as feasible. 2) the eigen estimations of the shut circle framework numbering the computed PID controller must be altogether arranged on the left a large portion of the difficult plane at the picked working circumstance.

### III. SIMULATION RESULTS AND DISCUSSIONS

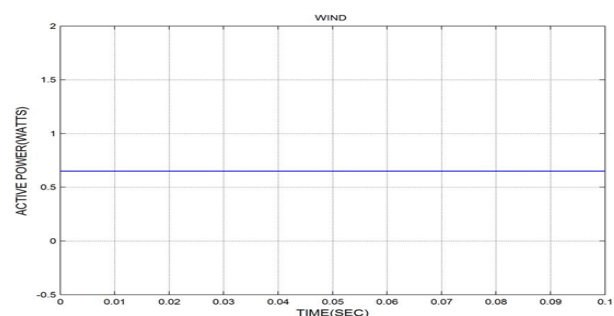


Fig.1. wind farm active power without statcom

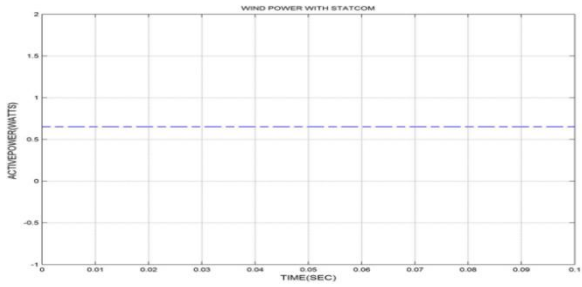


Fig.2.wind farm active power with statcom

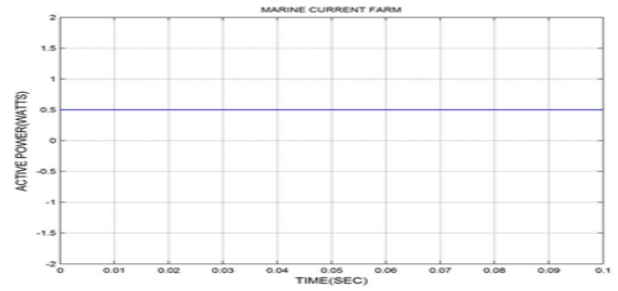


Fig.7.marine current farm active power without statcom

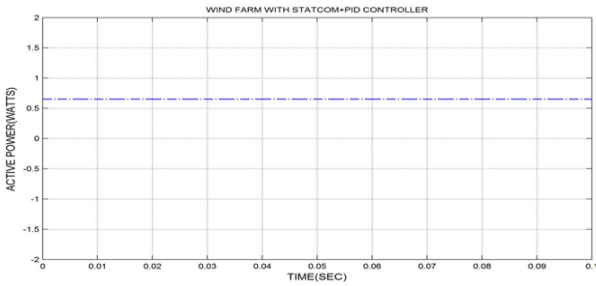


Fig.3.wind farm active power with statcom+PID controller

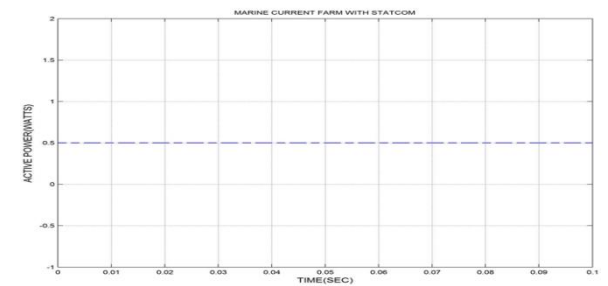


Fig.8.marine current farm active power statcom

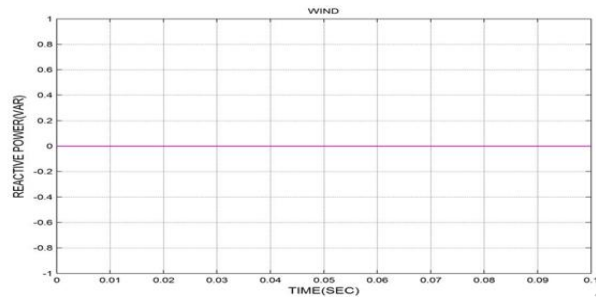


Fig.4.wind farm reactive power without statcom

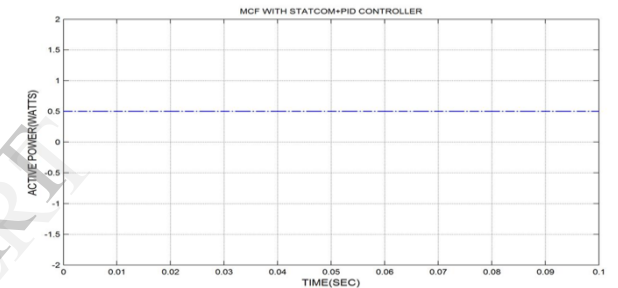


Fig.9.marine current farm active power with statcom+pid controller

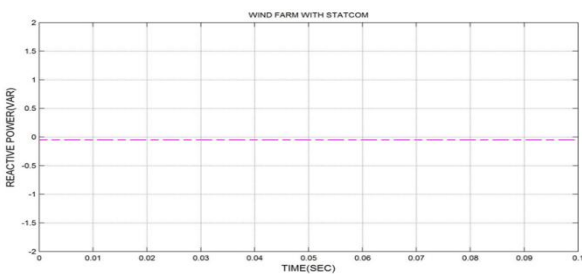


Fig.5.wind farm reactive power with statcom

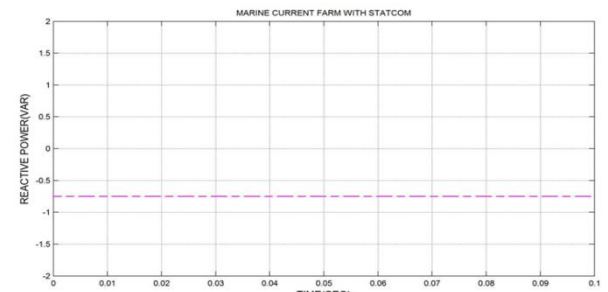


Fig.10.marine current farm reactive power without statcom

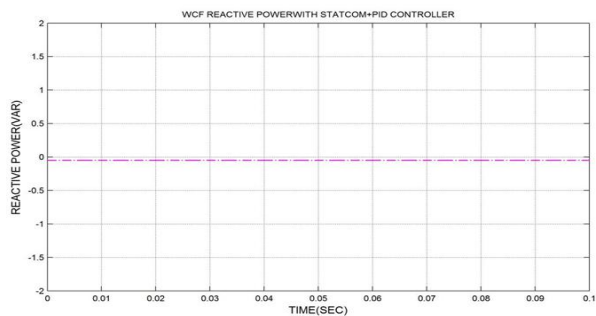


Fig.6.wind farm active power with statcom+pid controller

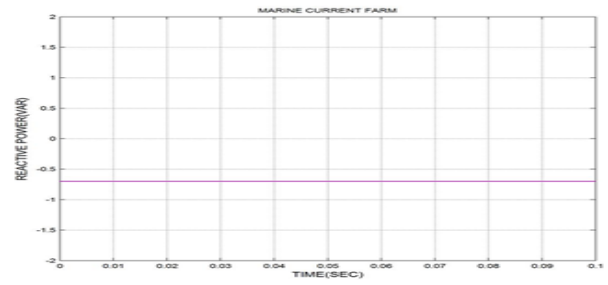


Fig.11.marine current farm reactive power statcom

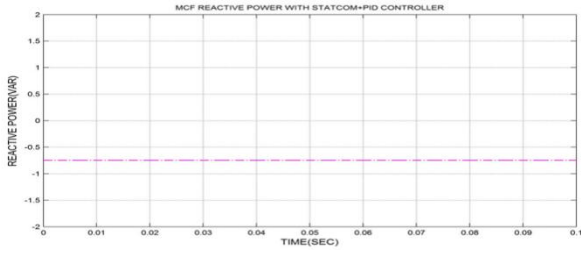


Fig.12.marine current farm reactive power with statcom+pid controller

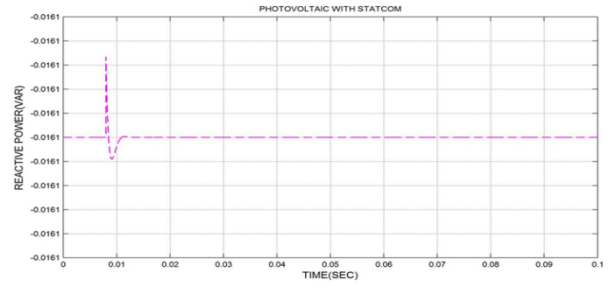


Fig.17.photovoltaic system reactive power with statcom

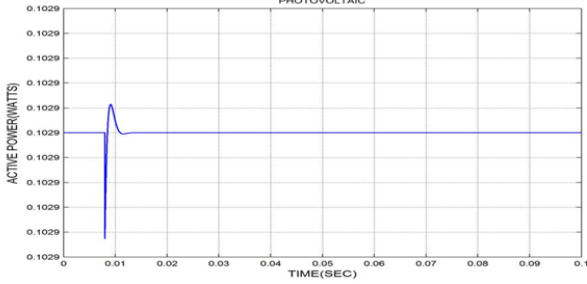


Fig.13.photovoltaic system active power without statcom

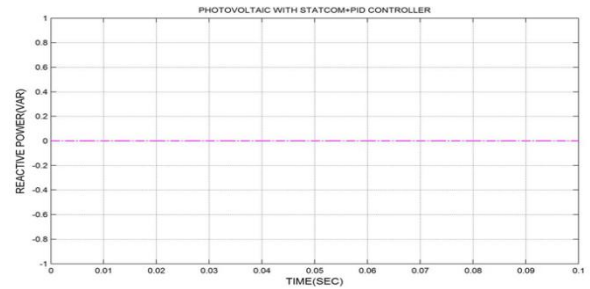


Fig.18.photovoltaic system reactive power with statcom+pid controller

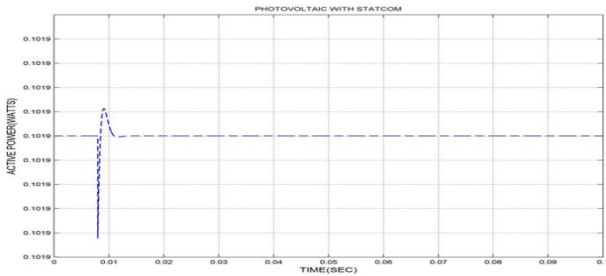


Fig.14.photovoltaic system active power with statcom

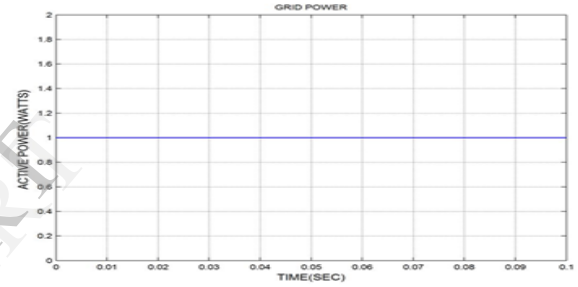


Fig.19.grid active power without statcom

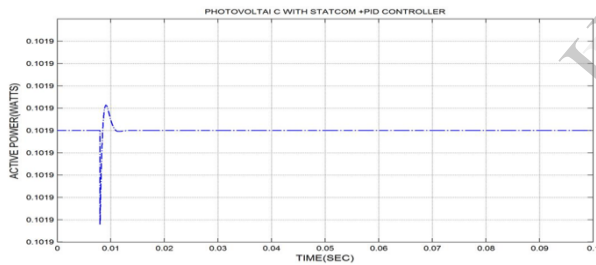


Fig.15.photovoltaic system active power with statcom+pid controller

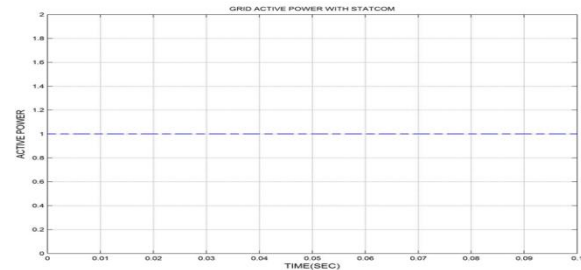


Fig.20.grid active power with statcom

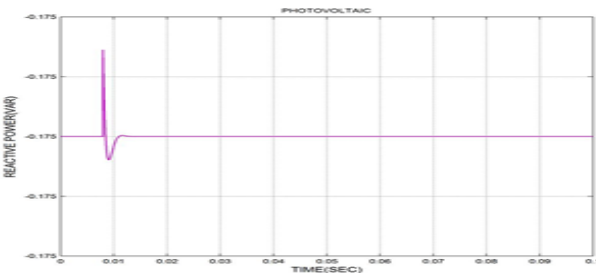


Fig.16.photovoltaic system reactive power without statcom

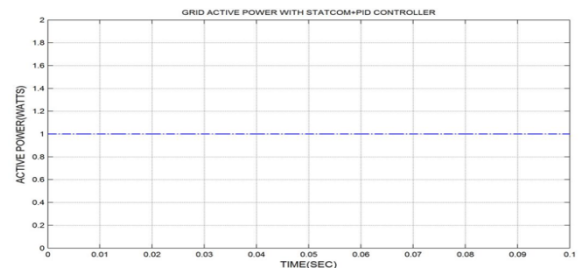


Fig.21.grid active power with statcom+pid controller



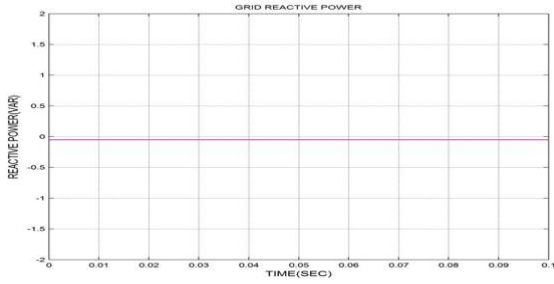


Fig.22.grid reactive power without statcom

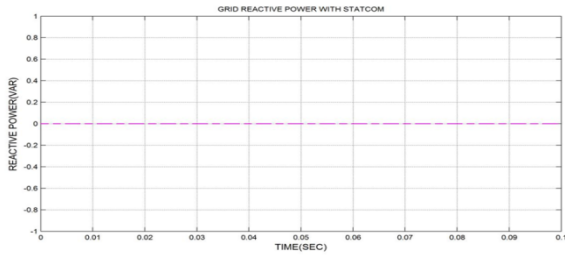


Fig.23.grid reactive power with statcom

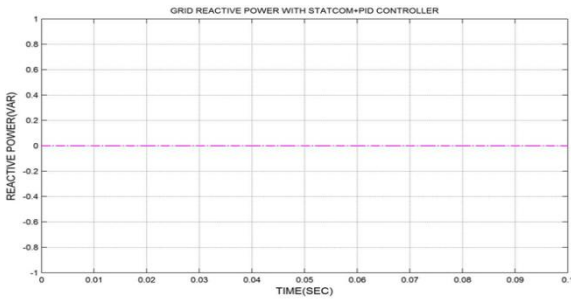


Fig.24.grid reactive power with statcom+pid controller

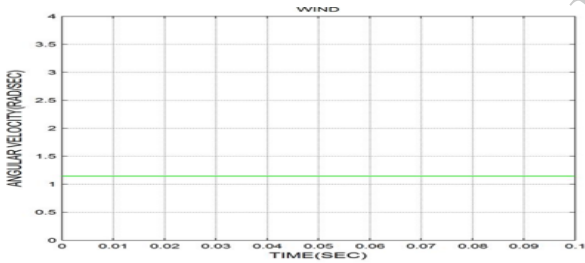


Fig.25.wind farm angular velocity without statcom

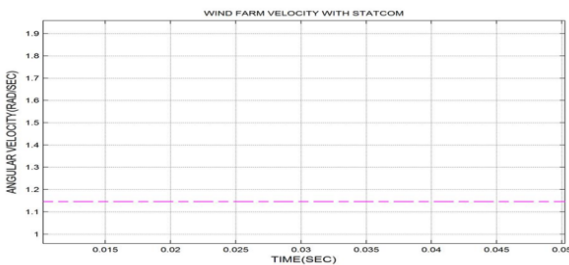


Fig.26.wind farm angular velocity with statcom

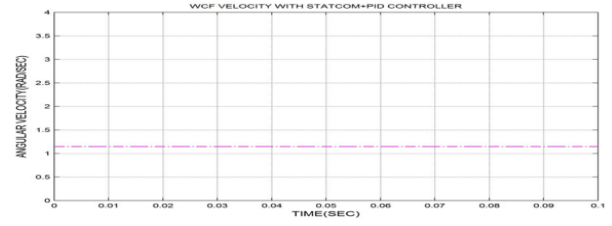


Fig.27.wind farm angular velocity with statcom+pid controller

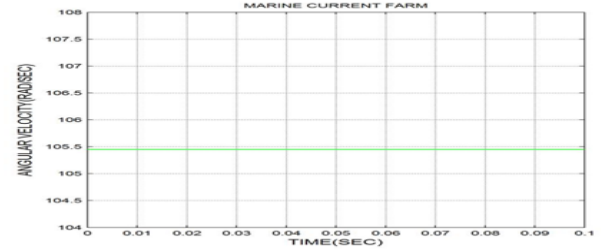


Fig.28.marine current farm angular velocity without statcom

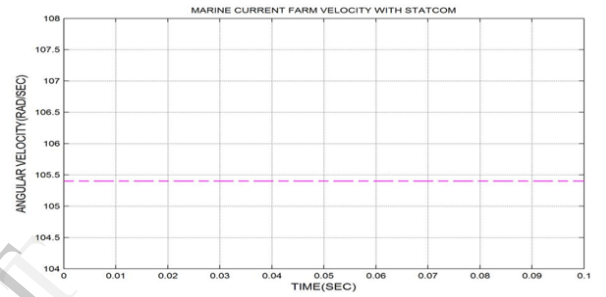


Fig.29.marine current farm angular velocity with statcom

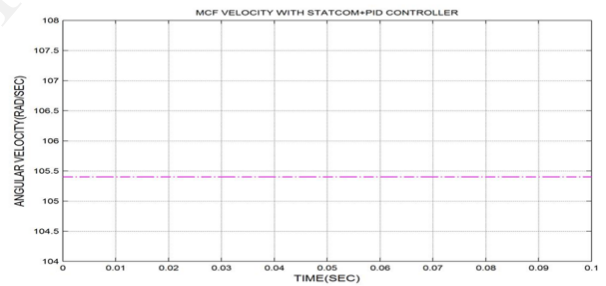


Fig.30.wind farm angular velocity with statcom+pid controller

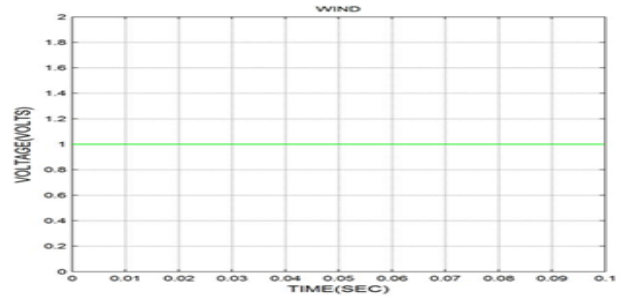


Fig.31.wind farm bus voltage without statcom

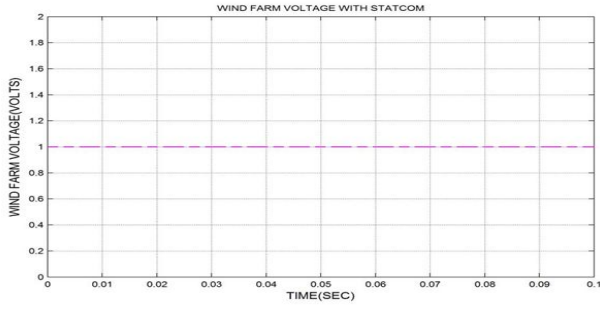


Fig.32.wind farm bus voltage with statcom

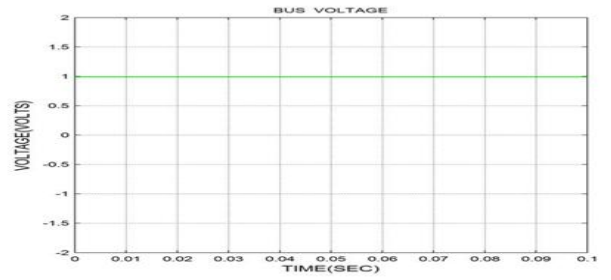


Fig.36.bus voltage without statcom

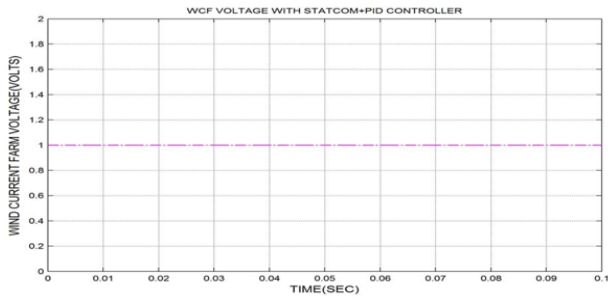


Fig.33.wind farm bus voltage with statcom+pid controller

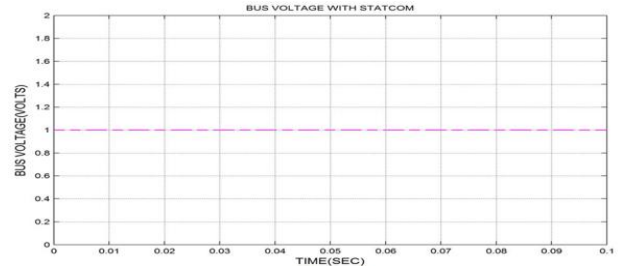


Fig.37.bus voltage with statcom

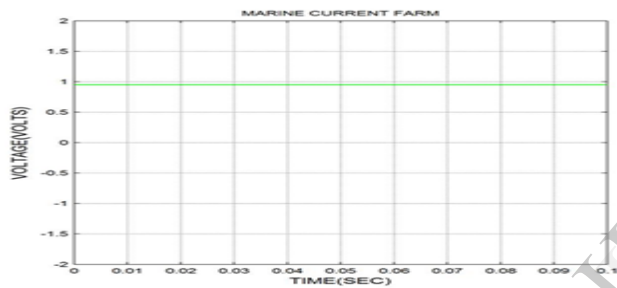


Fig.34.marine current farm bus voltage without statcom

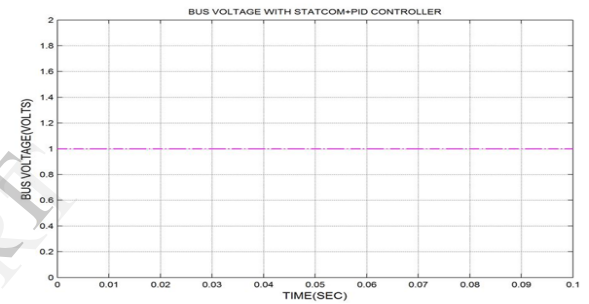


Fig.38.bus voltage with statcom+pid controller

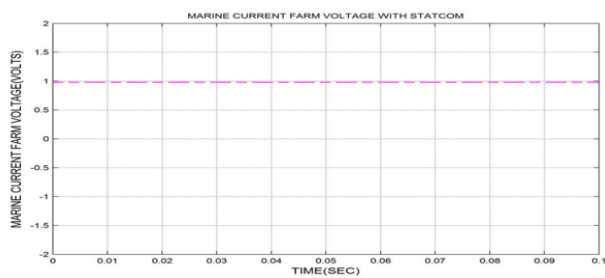


Fig.35.marine current farm bus voltage with statcom

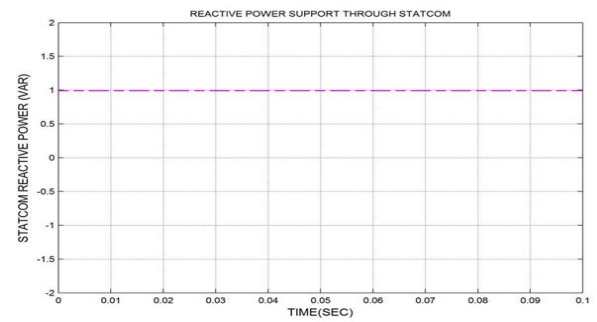


Fig.39.reactive power support to the grid by statcom

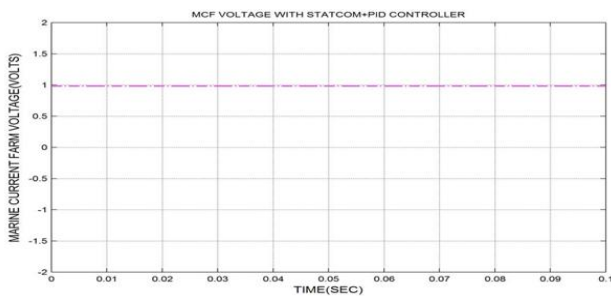


Fig.36.marine current farm bus voltage with statcom+pid controller

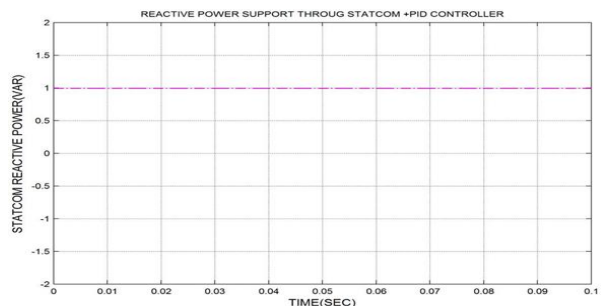


Fig.40.reactive power support to the grid by statcom+pid controller

## CONCLUSION

This exploration project has conceivable the change transient soundness of a fused OWF, MCF and PV schema with a Facts (STATCOM). A PID regulator has been gotten prepared on behalf of the STATCOM by strategy for a bound together come within reach of centered roughly post errand approach. Eigen regard estimations and time-space entertainments of the inspected skeleton theme to a sound wind-speed bothering, a marine current pace impediment, and a 3 stage short out blemish at the lattice have been experimentally carry out to express the gainfulness of the organized STATCOM connected among the orchestrated PID regulator on smothering voltage flimsiness of the considered structure and edifying scheme transient unflinching quality under diverse working situation. It could be accomplished from the reenactment happens that the masterminded STATCOM attached among the orchestrated PID regulator is fit for acculturating the presentation of the pondered consolidated OWF, MCF and PV structure below one of a kind working conditions.

## REFERENCES:

- [1] Li Wang, Senior Member, IEEE, and Chia-Tien Hsiung "Dynamic Stability Improvement of an Integrated Grid-Connected Offshore Wind Farm and Marine-Current Farm Using a STATCOM. *Power Syst* vol. 26, no. 2, may2011
- [2] S. E. B. Elghali, R. Balme, K. L. Saux, M. E. H. Benbouzid, J.F. Charpentier, and F. Hauville, "A simulation model for the evaluation of the electrical power potential Harnessed by a marine current turbine," *IEEE J.Ocean. Eng.*, vol. 32, no. 4, pp. 786–797, Oct. 2007.
- [3] W. M. J. Batten, A. S. Bahaj, A. F. Molland, and J. R. Chaplin, "Hydrodynamics of marine current turbines," *Renewab. Energy*, vol. 31, no. 2, pp. 249–256, Feb. 2006.
- [4] L. Myers and A. S. Bahaj, "Simulated electrical power potential harnessed by marine current turbine arrays in the alderney race," *Renewab. Energy*, vol. 30, no. 11, pp. 1713–1731, Sep. 2005.
- [5] H. Chong, A. Q. Huang, M. E. Baran, S. Bhattacharya, W. Litzemberger, L. Anderson, A. L. Johnson, and A. A. Edris, "STATCOM impact study on the integration of a large wind farm into a weak loop power system," *IEEE Trans. Energy Convers.*, vol. 23, no. 1, pp. 226–233, Mar. 2008.
- [6] H. Gaztanaga, I. Etxeberria-Otadui, D. Ocnasu, and S. Bacha, "Real-time analysis of the transient response improvement of fixed speed wind farms by using a reduced scale STATCOM prototype," *IEEE Trans. Power Syst.*, vol. 22, no. 2, pp. 658–666, May 2007.
- [7] K. R. Padiyar and N. Prabhu, "Design and performance evaluation of subsynchronous damping controller with STATCOM," *IEEE Trans. Power Del.*, vol. 21, no. 3, pp. 1398–1405, Jul. 2006.
- [8] W. L. Chen and Y. Y. Hsu, "Controller design for an induction generator driven by a variable speed wind turbine," *IEEE Trans. Energy Convers.*, vol. 21, no. 3, pp. 635–625, Sep. 2006.
- [9] A. Jain, K. Joshi, A. Behal, and N. Mohan, "Voltage regulation with STATCOMs: Modeling, control and results," *IEEE Trans. Power Del.*, vol. 21, no. 2, pp. 726–735, Apr. 2006.
- [10] B. Blaz'ic and I. Papic, "Improved D-STATCOM control for operation with unbalanced currents and voltages," *IEEE Trans. Power Del.*, vol. 21, no. 1, pp. 225–233, Jan. 2006.
- [11] A. H. Norouzi and A. M. Sharaf, "Two control schemes to enhance the dynamic performance of the STATCOM and SSSC," *IEEE Trans. Power Del.*, vol. 20, no. 1, pp. 435–442, Jan. 2005.
- [12] K. V. Patil, J. Senthil, J. Jiang, and R. M. Mathur, "Application of STATCOM for damping torsional oscillations in series compensated AC system," *IEEE Trans. Energy Convers.*, vol. 13, no. 3, pp. 237–243, Sep. 1998.
- [13] N. Mithulananthan, C. A. Canizares, J. Reeve, and G. J. Rogers, "Comparison of PSS, SVC, and STATCOM controllers for damping power system oscillations," *IEEE Trans. Power Syst.*, vol. 18, no. 2, pp. 786–792, May 2003.
- [14] P. Rao, M. L. Crow, and Z. Yang, "STATCOM control for power system voltage control applications," *IEEE Trans. Power Del.*, vol. 15, no. 4, pp. 1311–1317, Oct. 2000.
- [15] Y. Ye, M. Kazerani, and V. H. Quintana, "Current source converter based STATCOM: Modeling and control," *IEEE Trans. Power Del.*, vol. 20, no. 2, pp. 795–800, Apr. 2005.
- [16] Z. Yang, C. Shen, L. Zhang, M. L. Crow, and S. Atcitty, "Integration of a STATCOM and battery energy storage," *IEEE Trans. Power Syst.*, vol. 16, no. 2, pp. 254–260, May 2001.
- [17] R. Grinbanm, P. Halvarsson, D. Larsson, and P. R. Jones, "Conditioning of power grids serving offshore wind farms based on asynchronous generator," in *Proc. Conf. Power Electronics, Machine and Drives*, Mar./Apr. 2004, vol. 1, pp. 34–39.
- [18] P. M. Anderson and A. Bose, "Stability simulation of wind turbine system," *IEEE Trans. Power App. Syst.*, vol. PAS-102, pp. 3791–3795, Dec. 1983.
- [19] J. G. Slootweg, H. Polinder, and W. L. Kling, "Representing wind turbine electrical generating systems in fundamental frequency simulations," *IEEE Trans. Energy Convers.*, vol. 18, no. 4, pp. 516–524, Dec. 2003.
- [20] D. J. Trudnowski, A. Gentile, J. M. Khan, and E. M. Petritz, "Fixed-speed wind-generator and wind-park modeling for transient stability studies," *IEEE Trans. Power Syst.*, vol. 19, no. 4, pp. 1911–1917, Nov. 2004.
- [21] S. M. Mueen, M. H. Ali, R. Takahashi, T. Murata, J. Tamura, Y. Tomaki, A. Sakahara, and E. Sasano, "Transient stability analysis of wind generator system with the consideration of multi-mass shaft model," in *Proc. Int. Conf. Power Electronics and Drives Systems*, Jan. 16–18, 2006, vol. 1, pp. 511–516.